

A New Method for Density Gradient Measurements in Compressible Flows

J. Stricker*

Technion—Israel Institute of Technology, Haifa, Israel

and

O. Kafri†

Nuclear Research Center, Beer-Sheva, Israel

We suggest the use of a new method, moire deflectometry, for analysis of density gradients in compressible flows. This method, which is simpler to apply than schlieren and does not need precalibration, is capable of providing a fully quantitative diagnosis and map of the density gradient field. We demonstrate the method by a quantitative example of a two-dimensional diamond airfoil in a supersonic wind tunnel and compare it with other diagnostic methods widely used today.

Introduction

THE analysis of density distribution in compressible flows is of major importance in aerodynamics. Among the known methods for density measurements three are commonly used: interferometry, schlieren, and shadowgraphy. Each method is sensitive to a different density derivative. The readings in interferometry are proportional to the density, those in schlieren to the density gradients, and those in shadowgraphy to the Laplacian of the density. Although the most quantitative method is interferometry, it is only seldom applied. This is due to the severe mechanical stability requirements, about $\lambda/10$, which dictate the use of either very heavy equipment to carry the optical components or short laser pulses. The most popular method is schlieren photography, which is a rather simple real-time method, and is more sensitive than shadowgraphy.

The purpose of this paper is to demonstrate a new method, moire deflectometry, which was suggested recently,¹ for the analysis and mapping of density gradient fields in supersonic wind tunnels. The method, which is based on moire effect, is capable of measuring the deflection of rays of a collimated light beam. The optical system consists of a collimated light source, of the type used in schlieren photography, and two gratings, G_1 and G_2 , as shown schematically in Fig. 1. The moire pattern may be observed on a mat screen, S , attached to the grating G_2 . The two gratings, G_1 and G_2 , are oriented at an angle θ to each other, so that the resultant moire pattern consists of straight fringes separated by a distance P' given by²

$$P' = \frac{P}{2\sin(\theta/2)} \quad (1)$$

where P is the pitch of the gratings. The gratings are separated by a distance Δ , which should be adjusted so that the fringes appear sharp and the blur, due to diffraction, is minimized.³ It has been shown¹ that when a fringe is shifted from its original straight line position, at a point (Y_j, Z_k) (see Fig. 2) by an amount $h_{j,k}$, the deflection of the light ray, toward the Y direction, at the point $(Y_j, Z_k + h_{j,k})$ is

$$\phi_{j,k} = \frac{2h_{j,k}\sin(\theta/2)}{\Delta} \quad (2)$$

For small deflections, the angle $\phi_{j,k}$ is related to the refractive index n via

$$\phi_{j,k} = \frac{1}{n_f} \int_0^{x_f} \left(\frac{\partial n}{\partial y} \right)_{(Y_j, Z_k)} dx \quad (3)$$

where x is the space coordinate along the beam direction, and the subscript f denotes values at the end of the phase object. From Eqs. (2) and (3) one may obtain information similar in nature to that of schlieren photography. Moreover, this information is fully quantitative.

In fact, the moire deflectometry method makes use of only part of schlieren photography setup, namely, the collimated light source. Only two Ronchi rulings and a screen are required in addition (simple transparent mat paper is

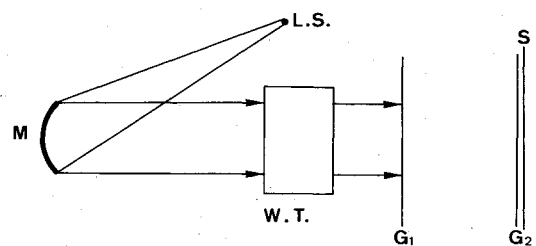


Fig. 1 Schematics of the experimental setup. L.S. is a point light source (may be a focused laser beam), M is a parabolic mirror, W.T. is the test section of the wind tunnel, G_1 and G_2 are Ronchi rulings, and S is a mat transparent screen.

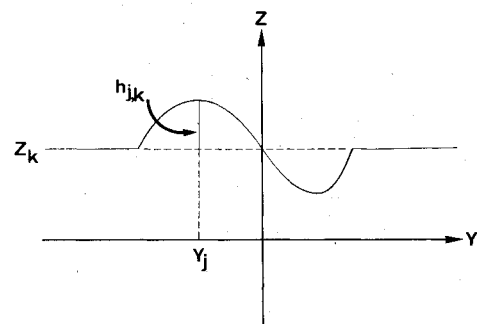


Fig. 2 Distorted line of a moire pattern. The distance $h_{j,k}$ is simply related by Eq. (2) to the deflection of the light ray at the location $(Y_j, Z_k + h_{j,k})$ in the Y direction.

adequate). The stability requirements are as tolerant as in shadowgraphy and are thus much easier to meet compared to those of interferometry. The suggested system is easy to align and low cost optics can be used. The sensitivity can be controlled merely by changing the distance between the gratings. The spatial resolution may be governed by changing the angle of rotation θ and the pitch of the gratings.

Experiment

In order to demonstrate the application of moiré deflectometry in aerodynamics, we used this method in supersonic wind tunnel experiments. The supersonic tunnel,⁴ with a test section of 40×50 cm, was designed for continuous Mach number variation, from $M=1.5$ to 4.0 by a single jack flexible nozzle. The model was held by a mount in such a way that its angle of attack could be varied between -20 and $+20$ deg. Two 60×50 -cm windows were mounted on the test section side walls. In each experiment both the stagnation pressure and the static pressure are measured, from which the Mach number is calculated.⁵ In all of the experiments the Mach number was 1.98 , the stagnation pressure $P_{st}=3.15$ atm, and the static pressure $p=0.415$ atm. The deflectometer, shown in Fig. 1, consists of a schlieren mirror with a 32 -cm diameter and 240 -cm focal length. Both a mercury lamp, as in the original schlieren system, and a 25 -mW cw He-Ne laser were used as light sources. Although the laser source yields a fringe pattern with a higher contrast, very good results were also obtained with the mercury lamp.

The model tested was a two-dimensional diamond profile airfoil, spanning the test section. Dimensions of the airfoil are given in Fig. 3. The airfoil was held at a zero angle of attack.

Results and Discussion

The ideal inviscid flow pattern of the airfoil is shown in Fig. 3. Flow over the upper surface is first compressed by an oblique shock wave, then turned through an expansion fan centered at the airfoil shoulder. The flow over the lower surface is symmetrical and therefore is not shown in the figure.

In Fig. 4 we present four photographs. Figure 4a is the geometrical shadow of the airfoil profile in a static deflectometry system, prior to wind tunnel operation. Figure 4b is the deflectogram of the model with flow. Figure 4c is the same as Fig. 4b but with an orthogonal fringe axis, so that

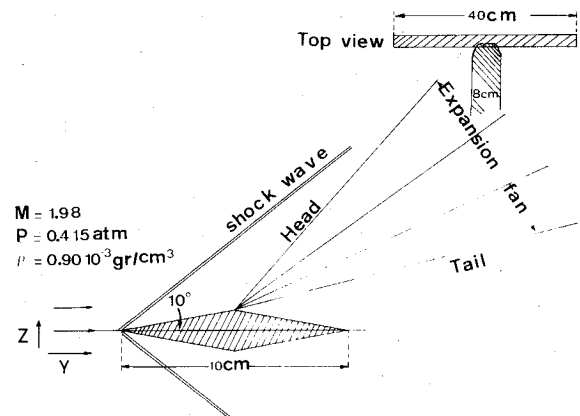


Fig. 3 Inviscid flow pattern of a two-dimensional diamond profile airfoil. Mach number of the free flow is $M=1.98$.

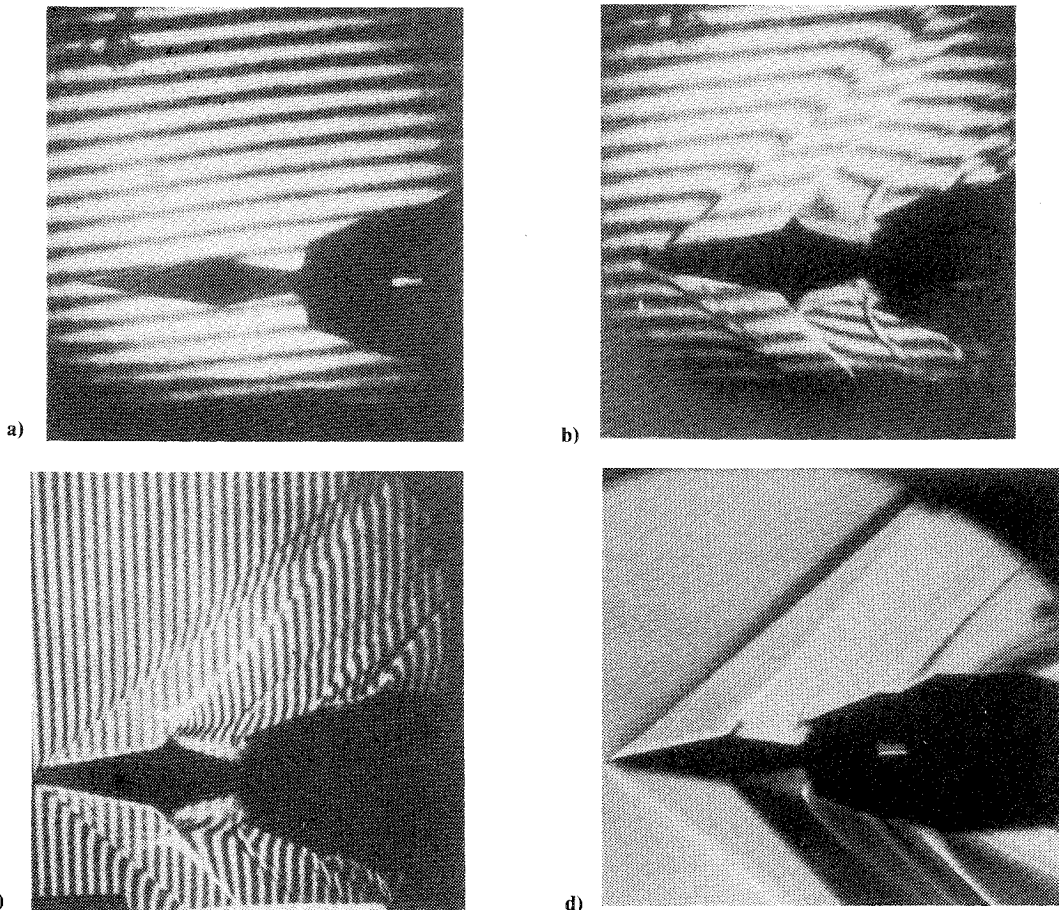


Fig. 4 Two-dimensional airfoil, shown in Fig. 3, in the supersonic wind tunnel. $M=1.98$, $P=0.415$ atm, and $\rho=0.90 \times 10^{-3} \text{ g/cm}^3$. Angle of attack is $\alpha=0$. a) Geometrical shadow of the airfoil in the deflectometer, without flow. The straight lines are the moiré fringes. b) Deflectogram of the model with flow. c) Same as in b but with perpendicular fringes. d) Schlieren photograph, with the same flow conditions as in b and c.

deflections in the Y direction measure gradients in the Z direction. The separation between the fringes in Fig. 4c is smaller than in Fig. 4b because of a larger angle θ [see Eq. (1)]. In Fig. 4d a schlieren photograph with the same flow conditions as in Figs. 4b and 4c is presented for comparison. In Fig. 5 the undisturbed moire pattern (Fig. 4a) is superimposed on the deflectogram of the model with flow (Fig. 4b). The deviation of the fringes from the original straight lines yields, via Eq. (3), information about the index of refraction gradients and therefore also about density gradients. The relation between density ρ and the index of refraction is given by⁶

$$n - 1 = 0.227\rho \quad (4)$$

or

$$\frac{\partial n}{\partial y} = 0.227 \frac{\partial \rho}{\partial y} \quad (5)$$

where ρ is in g/cm^3 . The gratings used were two Ronchi rulings with a pitch of $P = 0.0308$ cm; the angle θ was calculated from Eq. (1), by using the measured distance $P' = 1.001$ cm, to be $\theta = 3.053 \times 10^{-2}$ rad. The distance Δ was chosen, according to the density gradients expected, to be $\Delta = 18.0$ cm. Assuming that $\partial\rho/\partial y$ is constant along the x axis, it was calculated from Eqs. (2), (3), and (5) that a fringe deviation of 1 cm is equivalent to a density gradient of 0.884×10^{-4} g/cm^4 . In order to determine local density gradients from the deflectogram, one should be able to relate the distorted fringes to the original undisturbed ones. As seen in Fig. 5, this is not trivial in some cases. This problem can be solved in two different ways:

1) Since the deflectogram is a real-time measurement, one can observe the evolution of the fringe pattern at earlier stages where the gradients were smaller.

2) By gradually reducing the sensitivity of the deflectometer so as to observe smaller fringe deviations.

A comparison between calculated and measured density gradients at seven points along the expansion fan head was performed. The angular density gradient $\partial\rho/\partial\alpha$ at the head is calculated to be 0.688×10^{-3} $\text{g/cm}^3 \text{ rad}^{-1}$. The linear gradient in the fringe direction Y was calculated according to

$$\frac{\partial \rho}{\partial y} = \frac{\partial \rho}{\partial \alpha} \frac{\cos \beta}{r} \quad (6)$$

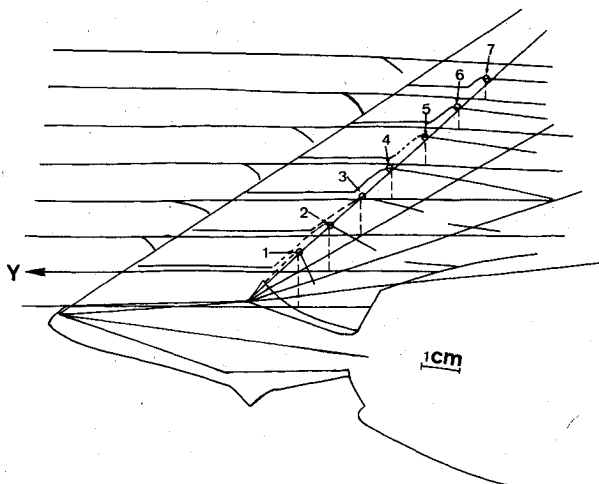


Fig. 5 Superposition of the fringes obtained in flow (Fig. 4b) with the undisturbed moire pattern (Fig. 4a). At the marked points, density gradients were calculated from the length of the broken lines. The lines, representing the shock front and the head and tail of the expansion fan, are inclined to flow axis by angles calculated from the ideal model (the same angles as in Fig. 3).

where r is the distance from the fan center and β is the angle between the fringe axis and the normal to the Mach line of the fan head. In this case $\beta = 0.943$ rad. The theoretical values of the ideal model vs the measured results are listed in Table 1. As one may see from the table, only in point 1 is there a significant deviation of experiment from theory. This is because this point is located in a region close to the holder where a turbulent separation bubble exists. In this region the flow does not expand as strongly as the nonviscid flow theory predicts, so that density gradients are smaller. At greater distances the effect of the holder is smaller and the observed flow follows more closely the ideal flow. The existence of the separation bubble is clearly seen in both the deflectograms and in the schlieren photograph.

Although the purpose of this paper is not to analyze in detail the aerodynamics of this model, we will point out some of the flow features that may be observed from the deflectogram.

1) It may be seen, both from the deflectogram and from the schlieren photograph, that the shock wave is not as sharp as may be expected, but is rather diffusive. It is clearly observed from the deflectogram that a pressure buildup exists ahead of the shock front. This effect is probably due to the interaction between the shock wave and the boundary layer developed on the windows of the test section.

2) As may be seen from Fig. 5, a small constant density gradient of about 2×10^{-5} g/cm^4 in the Y direction exists in the region between the shock wave and the expansion fan. Such a gradient does not exist theoretically. This is probably due to the decrease in the rate of the boundary-layer growth downstream from the airfoil leading edge. This effect is not observed in the schlieren photograph.

3) Behind the theoretical expansion fan, close to the model, one may observe blurred fringes and considerable contrast reduction. This is an indication of a turbulent flow region. This effect is not observed in our schlieren photograph.

Table 1 Comparison of theoretical and experimental density gradients, in the Y direction, at different points on the expansion fan head. All values are in units of 10^{-4} g/cm^4 . The points are marked in Fig. 5

Point No.	Theoretical	Measured
1	4.23	2.77
2	2.74	2.25
3	1.95	1.86
4	1.58	1.47
5	1.27	1.35
6	1.07	0.97
7	0.94	0.97

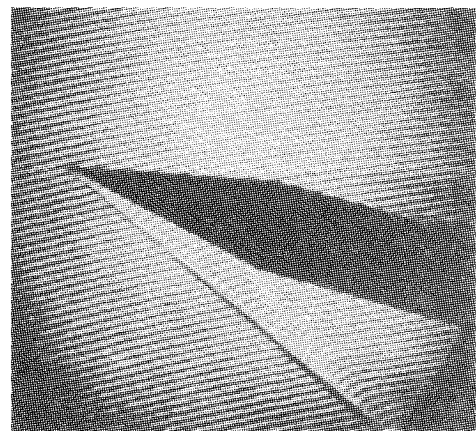


Fig. 6 Deflectograms of a 23-deg circular cone in the supersonic wind tunnel at an angle of attack $\alpha = 15$ deg. Flow conditions: $M = 1.98$, $P = 0.415$ atm, and $\rho = 0.90 \times 10^{-3}$ g/cm^3 .

4) The shadow of the model is larger than the geometrical one. This effect is probably due to very high density gradients in the boundary layers which remove the light rays from the object (lens effect).

Additional experiments with axisymmetric bodies were performed. Figure 6 shows a deflectogram of a circular cone in the supersonic flow at an angle of attack $\alpha = 15$ deg. The conical shock attached to the apex of the cone and the expansion fans centered at the shoulder are clearly observed. For such objects at an angle of attack $\alpha = 0$ deg the analysis of density gradients requires Abel transformation.⁷ However, such an analysis is not within the scope of this paper.

Summary

In this paper we suggest the use of moiré deflectometry as a diagnostic method for transonic and supersonic wind tunnels. In many aspects this method is similar to schlieren. Both methods are sensitive to density gradients and have the same mechanical stability requirements. However, our method has several advantages over schlieren photography:

- 1) The experimental setup is simpler. In fact, only a collimated beam and two Ronchi rulings are required.
- 2) This method is as quantitative as interferometry and yields an optical mapping of the field.
- 3) The method is capable of observing turbulence from the reduction in fringe contrast.
- 4) This method does not need precalibration. All calculated quantities are absolute and do not require any calibration references.

This method differs from interferometry in the measured property, namely, density gradient instead of density. In wind tunnel experiments density gradients are generally of greater

interest and more convenient when Abel transformation is applied. The advantages over interferometry follow:

- 1) Stability requirements of the system are determined by the measurement sensitivity rather than by $\sim \lambda/10$, as required by interferometry.
- 2) The sensitivity is easily tuned by simply varying the distance between the gratings.
- 3) Incoherent white light may be used.

Acknowledgments

We thank Professor A. Seginer and Dr. A. Brosh for useful discussions and for making available the facilities of the Technion's wind tunnel. We also thank J. Sasson for technical assistance.

References

- ¹Kafri, O., "Noncoherent Method for Mapping of Phase Objects," *Optics Letters*, Vol. 5, Dec. 1980, pp. 555-557.
- ²Kafri, O. and Livnat, A., "Tunable Grating for Moiré Mapping," *Optics Letters*, Vol. 4, Oct. 1979, pp. 314-316.
- ³Durell, A. J. and Parks, V. J., *Moiré Analysis of Strain*, Prentice-Hall, New Jersey, 1970.
- ⁴Kadushin, I. and Rom, J., "Design of an Intermittent, Single-Jack Flexible Nozzle Supersonic Wind-Tunnel for Mach Numbers 1.5 to 4.0," Dept. of Aeronautical Engineering, Technion, I.I.T., Haifa, Israel, T.A.E. Rept. 86, 1968.
- ⁵Shapiro, A. H., *The Dynamics and Thermodynamics of Compressible Fluid Flow*, Part I, The Ronald Press, New York, 1953.
- ⁶Weast, R. C., ed., *CRC Handbook of Chemistry and Physics* 1973-1974, 54th ed., CRC Press, Ohio, 1973.
- ⁷Bockasten, K., "Transformation of Observed Radiances into Radial Distribution of the Emission of Plasma," *Journal of the Optical Society of America*, Vol. 51, Feb. 1961, pp. 943-947.

From the AIAA Progress in Astronautics and Aeronautics Series...

EXPERIMENTAL DIAGNOSTICS IN GAS PHASE COMBUSTION SYSTEMS—v. 53

Editor: Ben T. Zinn; Associate Editors: Craig T. Bowman, Daniel L. Hartley, Edward W. Price, and James F. Skiffstad

Our scientific understanding of combustion systems has progressed in the past only as rapidly as penetrating experimental techniques were discovered to clarify the details of the elemental processes of such systems. Prior to 1950, existing understanding about the nature of flame and combustion systems centered in the field of chemical kinetics and thermodynamics. This situation is not surprising since the relatively advanced states of these areas could be directly related to earlier developments by chemists in experimental chemical kinetics. However, modern problems in combustion are not simple ones, and they involve much more than chemistry. The important problems of today often involve nonsteady phenomena, diffusional processes among initially unmixed reactants, and heterogeneous solid-liquid-gas reactions. To clarify the innermost details of such complex systems required the development of new experimental tools. Advances in the development of novel methods have been made steadily during the twenty-five years since 1950, based in large measure on fortuitous advances in the physical sciences occurring at the same time. The diagnostic methods described in this volume—and the methods to be presented in a second volume on combustion experimentation now in preparation—were largely undeveloped a decade ago. These powerful methods make possible a far deeper understanding of the complex processes of combustion than we had thought possible only a short time ago. This book has been planned as a means of disseminating to a wide audience of research and development engineers the techniques that had heretofore been known mainly to specialists.

671 pp., 6x9, illus., \$20.00 Member \$37.00 List

TO ORDER WRITE: Publications Dept., AIAA, 1290 Avenue of the Americas, New York, N.Y. 10019